

# Evaluation of Seismic Fragility of RC Frame Structure Using Vector-Valued Intensity Measures



Chao Xu & Zengping Wen

*Institute of Geophysics, China Earthquake Administration*

## SUMMARY:

The earthquake ground motion potential is commonly presented by an intensity measure (IM) in seismic fragility evaluation. Scalar-valued intensity measures usually could not describe the magnitude and distance dependences of ground motion characteristics that significantly affect variability of fragility assessment. Alternative vector-valued IMs comprised of two ground motion parameters were used to present the ground motion potential. All the vectors considered here are based on  $S_a(T_1)$  (spectral acceleration at the first mode period of vibration of the structure) as the first parameters. As the second parameter of the vector, the peak ground velocity (PGV) and spectral shape parameters  $R_{\eta, \xi}$  and  $N_p$  were considered. The sufficiency and efficiency of these IMs were studied for medial-story RC frame structures and vector-valued IM based fragility surfaces were developed. It is shown that fragility surfaces based on vector-valued IMs are better able to represent the damage potential of earthquake than fragility curves.

*Keywords: Fragility surface, vector-valued IMs, sufficiency and efficiency, Incremental dynamic analysis*

## 1. INTRODUCTION

The damage potential of earthquake ground motion is usually characterized by a ground motion parameter called the intensity measure (IM) in seismic vulnerability assessment. A good IM should meet the requirement of efficiency and sufficiency (Lucco, 2002). Efficiency means the ability to accurately predict the response of a structure subjected to earthquakes (i.e., small dispersion of structural response subjected to earthquake ground motions for a given IM). And a sufficient IM is defined as one that renders structural responses subjected to earthquake ground motions for a given IM conditionally independent of other ground motion properties (i.e., no other ground motion information is needed to characterize the structural response). An efficient IM results in smaller variability of structural response, which implies fewer ground motion input for performance evaluation. Sufficiency of an IM is desirable because it reduces the complexity of record selection procedure based on seismic environment (i.e., magnitude, distance, site conditions, etc.)

In the past, peak ground acceleration (PGA) was commonly used as an IM. Simplicity is the main advantage of PGA, but it results in great dispersion of structural response. More recently, the spectral acceleration at the first mode vibration of the structure,  $S_a(T_1)$ , has been thoroughly studied and became very popular. This IM contains ground motion spectral information as well as dynamic character of structure, so it's more efficient and sufficient than PGA (Hwang HHM and Huo JR, 1990, 1994; Shinozuka M, et al., 2000). However, earthquake disaster experience and strong ground motion data show that the structural seismic response depends on ground motion amplitude, spectrum, and duration characteristics simultaneously, and the different combinations of these three elements determine the degree of safety of the structure. Numerous studies also showed that scalar-valued IM such as  $S_a(T_1)$  couldn't comprehensively describe the complex nature of earthquake ground motions, resulting in great uncertainty in vulnerability assessment (Hanks TC and McGuire RK, 1981; Shome N, et al., 1998; Song J and Ellingwood BR, 1999; Ellingwood BR, 2001; Kafali C and Grigoriu M,

2004; Schotanus MIJ, et al., 2004). In order to accurately characterize the ground motion potential, some researchers promote the use of vector-valued IMs and some progress has been made (Cordova, P.P, et al., 2001; Baker JW and Cornell CA, 2004, 2005; Luco N, et al., 2005; Kafali C and Grigoriu M, 2007; Rajeev P, et al., 2008; Sei'ichiro Fukushima, 2010; D.M.Seyedi, et al., 2010).

Although previous researchers have shown that using vector-valued IMs can lead to a better prediction of the structural damage, very few have gone the extra step to develop vector-valued IM based vulnerability functions. The aim of this paper is to evaluate the seismic vulnerability of medial-story RC frame structures by means of several vector-valued IMs. All the vectors considered here are based on  $S_a(T_1)$  (spectral acceleration at the first mode period of vibration of the structure) as the first parameters. As the second parameter of the vector, the peak ground velocity (PGV) and spectral shape parameters  $R_{T_1, T_2}$  and  $N_p$  were considered. The efficiency and sufficiency of these IMs were studied and vector-valued IM based fragility surfaces were developed. It is found that fragility surfaces based on vector-valued IM are better able to represent the damage potential of earthquake than fragility curves.

## 2 VECTOR-VALUED IMS SELECTED

The seismic fragility of the structure is evaluated using three different vector-valued ground motion IMs.  $S_a(T_1)$  is used as the main parameter (denote as IM<sub>1</sub>) of the vector-valued IMs because it has been found to be a good scalar-valued IM. The three vector-valued IMs are  $S_a(T_1) + R_{PGV, S_a}$ ,  $S_a(T_1) + R_{T_1, T_2}$  and  $S_a(T_1) + N_p$ , where the second parameters (denote as IM<sub>2</sub>) are defined as:

$$R_{PGV, S_a} = PGV / S_a(T_1) \quad (2.1)$$

$$R_{T_1, T_2} = S_a(T_2) / S_a(T_1) \quad (2.2)$$

$$N_p = S_{a, avg}(T_M, \dots, T_N) / S_a(T_1) \quad (2.3)$$

$$S_{a, avg}(T_M, \dots, T_N) = \left( \prod_{i=M}^N S_a(T_i) \right)^{1/(N-M+1)} \quad (2.4)$$

In Eqn. 2.1, PGV is used to study the impact of peak ground motion on structural response. The parameter  $R_{T_1, T_2}$  in Eqn. 2.2 is defined as the ratio between the spectral acceleration at period  $T_2$  divided by spectral acceleration at period  $T_1$ , as shown in Figure 2.1.

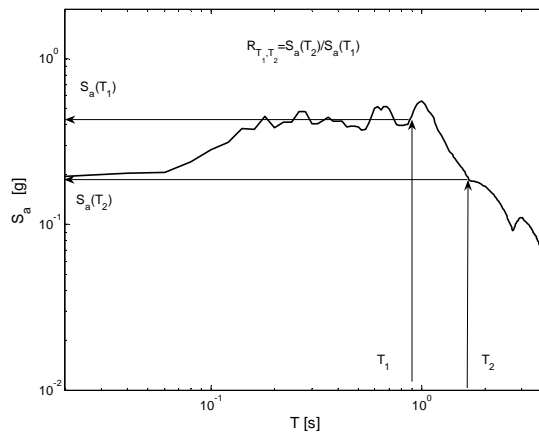


**Figure 2.1.** Calculation of  $R_{T_1, T_2}$  for a given response spectrum

The parameter  $Np$  is defined as the ratio between  $S_{a,avg}(T_M, \dots, T_N)$  divided by spectral acceleration at period  $T_1$ , where  $S_{a,avg}(T_M, \dots, T_N)$  is the geometric mean of spectral acceleration between an specific period range  $T_M$  to  $T_N$ , as shown in Eqn. 2.4.  $R_{\tau, \tau_2}$  and  $Np$  are representative of the spectral shape, which may account for the impact of higher mode effect and structural softening effect on structural response. Here, the normalization between  $S_a(T_1)$  let the second parameter be independent of the scaling level of the records based on  $S_a(T_1)$ .

### 3 STRUCTURAL MODEL AND GROUND MOTION RECORDS

#### 3.1 Structural Design Parameters

A regular RC frame structure of eleven-story was selected for case study. This frame was designed according to the Chinese Seismic Design Code (GB50011-2001) with the seismic fortification intensity of VII, design basic acceleration of ground motion if 0.15g and design characteristic period of ground motion of 0.3s. The structure has three bays of 7.2m and eleven stories. The height of the first story is 4.5s and other stories are 3.6m. The section dimensions of structural members and materials are list in Table 3.1.1 and average strength of the materials are list in Table 3.1.2.

**Table 3.1.1.** Section Dimensions and Materials of Structural Members

Story Number	Side Column (mm×mm)	Middle Column (mm×mm)	Beam (mm×mm)	Concrete	Steel Bar
1-6 Story	600×600	650×700	300×700	C30	HB335
7-11 Story	550×550	600×650	300×700	C30	HB335

**Table 3.1.2.** Average Strength of the Materials (N/mm<sup>2</sup>)

	Strength of C30	Elastic Modulus of C30	Strength of HB335	Elastic Modulus of HB335
Mean	26	32400	392	200000

#### 3.2 Nonlinear Dynamic Analysis Model

A modified version of the DRAIN-2DX (Prakash V, et al., 1993) program was used to create the finite element model and perform the nonlinear dynamic response history analysis. The structural components were modeled by beam-column element with plastic hinges. A 2% strain-hardening ratio was considered to model the cyclic behavior of the structural components. P-Δ effect was considered by adding a geometric stiffness matrix to the stiffness matrix of each element. Different yield surfaces were specified to beam members and column members to distinguish the different mechanic behaviors. The critical damping ratio was assumed to be 5%. The fundamental period of the structure is 1.6s according to modal analysis.

#### 3.3 Failure Criterion

Five damage states are adopted, that are undamaged, slight damage, moderate damage, intensive damage and collapse. And the maximum inter-story drift ratio is selected as damage measure. Based on a large number of experiment data of RC frames, Gao Xiaowang proposed the method for calculating threshold maximum inter-story drift ratio for the onset of slight damage, moderate damage, extensive damage and collapse states. Lognormal distribution was adopted to describe the threshold value. The mean values and coefficient of variation of threshold maximum inter-story drift ratios for

**Table 3.3.1.** Mean Values and Coefficient of Variation of Threshold Maximum Inter-story Drift Ratios

Damage States	Slight Damage	Moderate Damage	Extensive Damage	Collapse
Mean Value	1/350(0.0286%)	0.654%	1/80(1.25%)	3.6%
Coefficient of Variation	0.38	0.38	0.38	0.38

the five damage states are calculated. Results are shown in Table 3.3.1.

### 3.4 Ground Motions for Fragility Assessment

According to the recommendations of ATC-63, 40 ground motions records were selected to perform the fragility assessment. Several principles were followed in the record selection procedure as below:

(1) free-field records; (2) no pulse feature; (3) HP larger than 0.25Hz. Several important characteristics of the records are summarized in table 3.4.1.

**Table 3.4.1** Important Characteristics of the Records

Record	Event	Year	Mw	Station	PGA(g)	PGV(cm/s)
1	Imperial Valley-06	1979	6.53	Calipatria Fire Station	0.078	13.3
2	Imperial Valley-06	1979	6.53	Chihuahua	0.27	12.42
3	Imperial Valley-06	1979	6.53	Compuertas	0.186	6.91
4	Imperial Valley-06	1979	6.53	El Centro Array #1	0.139	15.84
5	Imperial Valley-06	1979	6.53	El Centro Array #12	0.116	21.8
6	Imperial Valley-06	1979	6.53	El Centro Array #13	0.139	13.0
7	Imperial Valley-06	1979	6.53	Niland Fire Station	0.109	11.87
8	Imperial Valley-06	1979	6.53	Plaster City	0.111	17.79
9	Imperial Valley-06	1979	6.53	Parachute Test Site	0.057	5.39
10	Imperial Valley-06	1979	6.53	Westmorland Fire Sta	0.11	21.89
11	Loma Prieta	1989	6.93	Agnews State Hospital	0.172	25.94
12	Loma Prieta	1989	6.93	Capitola	0.443	29.21
13	Loma Prieta	1989	6.93	Coyote Lake Dam (Downst)	0.16	13.04
14	Loma Prieta	1989	6.93	Gilroy Array #3	0.367	44.66
15	Loma Prieta	1989	6.93	Gilroy Array #4	0.212	37.86
16	Loma Prieta	1989	6.93	Gilroy Array #7	0.225	16.4
17	Loma Prieta	1989	6.93	Halls Valley	0.134	15.4
18	Loma Prieta	1989	6.93	Hollister Diff. Array	0.279	35.57
19	Loma Prieta	1989	6.93	Palo Alto - SLAC Lab	0.194	37.45
20	Loma Prieta	1989	6.93	Salinas - John & Work	0.112	15.68
21	Loma Prieta	1989	6.93	Sunnyvale - Colton Ave.	0.207	37.28
22	Northridge-01	1994	6.69	Arcadia - Arcadia Av	0.104	7.32
23	Northridge-02	1994	6.69	Baldwin Park - N Holly	0.123	8.17
24	Northridge-03	1994	6.69	Canoga Park - Topanga Can	0.42	60.69
25	Northridge-04	1994	6.69	Downey - Birchdale	0.171	8.12
26	Northridge-05	1994	6.69	Elizabeth Lake	0.109	8.96
27	Northridge-06	1994	6.69	Glendale - Las Palmas	0.206	7.39
28	Northridge-07	1994	6.69	LA - Centinela St	0.322	22.86
29	Northridge-08	1994	6.69	LA - Fletcher Dr	0.24	26.22
30	Northridge-09	1994	6.69	LA - N Faring Rd	0.273	15.8
31	Northridge-10	1994	6.69	LA - Pico & Sentous	0.186	14.23
32	Northridge-11	1994	6.69	LA - Saturn St	0.474	34.48
33	Northridge-12	1994	6.69	LA - Univ. Hospital	0.214	10.76
34	Northridge-13	1994	6.69	La Crescenta - New York	0.159	11.28
35	Northridge-14	1994	6.69	Lawndale - Osage Ave	0.153	7.95
36	San Fernando	1971	6.61	LA - Hollywood Stor FF	0.174	14.85
37	Superstitt Hills	1987	6.54	Brawley Airport	0.156	13.89
38	Superstitt Hills	1987	6.54	Calipatria Fire Station	0.247	14.54
39	Superstitt Hills	1987	6.54	Plaster City	0.186	20.62
40	Superstitt Hills	1987	6.54	Poe Road (temp)	0.446	35.71

## 4 EVALUATION OF SEISMIC FRAGILITY USING VECTOR-VALUED IMS

Seismic fragility assessment for the vector valued intensity measures is developed by incremental dynamic analysis (IDA) (Dimitrios Vamvatsikos and C.Allin Cornell, 2002) of the structure subject to

the records by using the first parameter of the vector  $IM_1$ , in this case  $S_a(T_1)$ , and then using log-linear regression model to account for the impact of the second parameter  $IM_2$ . Figure 4.1(a) shows IDA curves based on a vector valued intensity measure:  $S_a(T_1)$  and  $R_{T_1, T_2}(T_2 = 3.0s)$ . The point where each IDA curve first reaches maximum inter-story drift ratio of 1% (indicated by red circles) defined a set of IM capacity values. These points are plotted in Figure 4.1(b). It is apparent in Figure 4.1(b) that the  $S_a(T_1)$  capacity (denoted by  $S_a(T_1)_{cap}$ ) tends to be larger for smaller  $R_{T_1, T_2}(T_2 = 3.0s)$ , in other words, the structural response tends to be larger for larger  $R_{T_1, T_2}(T_2 = 3.0s)$  when records are scaled to a specific  $S_a(T_1)$  level, which means that  $R_{T_1, T_2}(T_2 = 3.0s)$  can explain part of the variation of  $S_a(T_1)$  capacity or variation of structural response. In Figure 4.1(b) the conditional distribution of  $\ln S_a(T_1)_{cap}$  appears to be linearly dependent upon  $\ln R_{T_1, T_2}(T_2 = 3.0s)$ , so log-linear regression can be used to find the conditional mean and standard deviation of  $\ln S_a(T_1)_{cap}$  given  $R_{T_1, T_2}(T_2 = 3.0s)$ , i.e.:  $\mu_{\ln S_a(T_1)_{cap}}$  and  $\beta_{S_a(T_1)_{cap}}$ . Then  $T_2$  is selected over arrange of possible values for  $R_{T_1, T_2}$  to maximum efficiency, or minimize  $\beta_{S_a(T_1)_{cap}}$ . A plot of fractional reduction in  $\beta_{S_a(T_1)_{cap}}$  (compared to scalar valued IM  $S_a(T_1)$ ) by  $R_{T_1, T_2}$  for different  $T_2$  values is shown in Figure 4.2, where the inter-story drift ratio demand is 1%. We see that the optimal  $T_2$  value is 2.4s, which can result in a minimum dispersion of  $\beta_{S_a(T_1)_{cap}}$ .

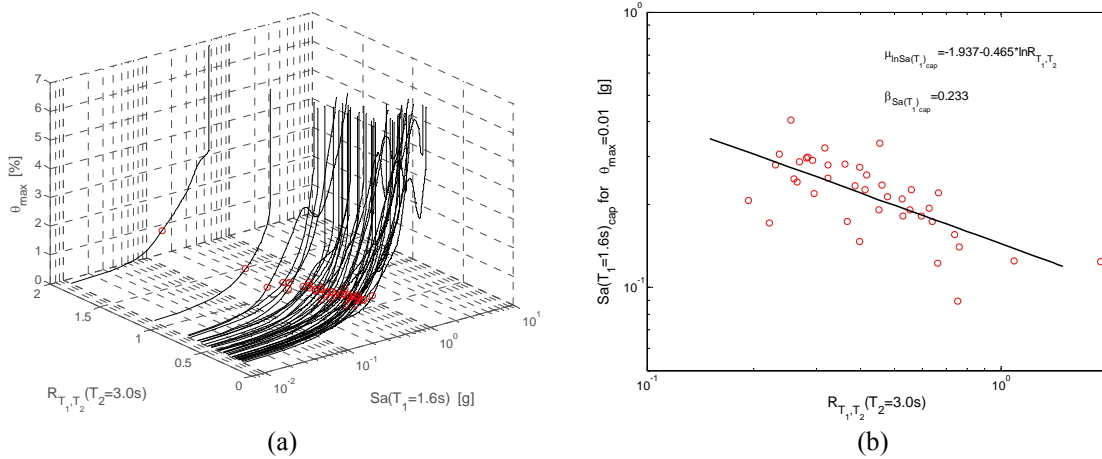


**Figure 4.1.** (a) Incremental dynamic analysis with a vector valued intensity measure,  $S_a(T_1)$  and  $R_{T_1, T_2}(T_2 = 3.0s)$ ; (b)  $S_a(T_1)$ ,  $R_{T_1, T_2}(T_2 = 3.0s)$  pairs as well as the log-linear regression result corresponding to occurrence of 1% maximum inter-story drift ratio

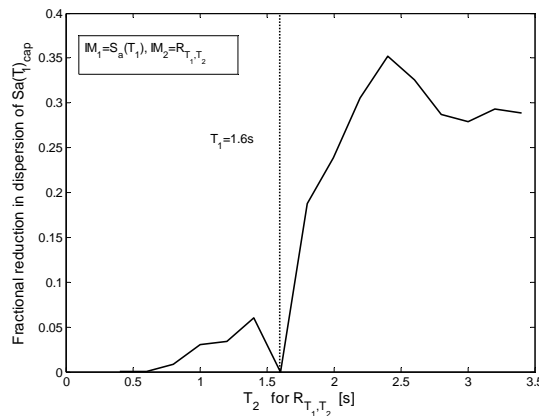


**Figure 4.2.** Fractional reduction in dispersion of  $S_a(T_1)_{cap}$  by  $R_{T_1, T_2}$  for  $T_2$  between 0.3s and 3.4s for a drift demand level of 1%

This optimal  $T_2$  value is only relevant for a single level of drift demand. We can repeat the same calculation to different levels of drift demand and shown the result in Figure 4.3. It is apparent that the optimal  $T_2$  value varies depending on the drift demand level. For lower drift demand level, for example  $\theta_{\max} = 0.001$ , we find that the optimal  $T_2$  is about 0.5s. This is near 0.54s: the second-mode period of vibration of the structure. For higher level of drift demand, for example  $\theta_{\max} \geq 0.01$ , we find that the optimal  $T_2$  is larger than  $T_1$ , here  $T_2=2.4$ s is the best choice. The above trend can be seen more clearly in Figure 4.4, which shows fractional reduction in dispersion of  $S_a(T_1)_{cap}$  vs drift demand level for  $T_2$  between 0.3s and 3.4s.

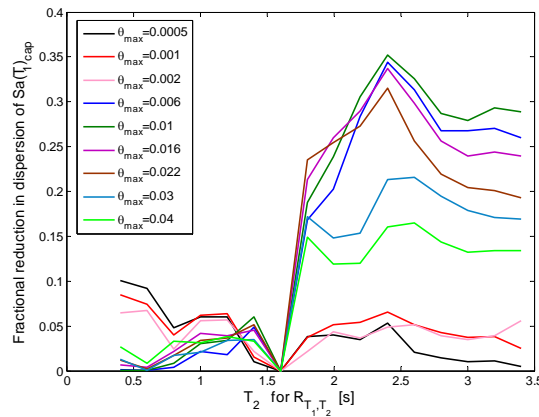


**Figure 4.3.** Fractional reduction in dispersion of  $S_a(T_1)_{cap}$  by  $R_{T_1,T_2}$  for  $T_2$  between 0.3s and 3.4s for different drift demand levels

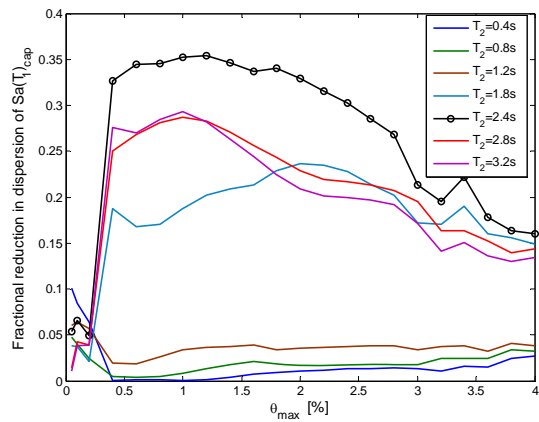


**Figure 4.4.** Fractional reduction in dispersion of  $S_a(T_1)_{cap}$  versus drift demand level for  $T_2$  between 0.3-3.4s

If one were to combine engineering intuition with the results of figure 4.2 and Figure 4.3, the following conclusion might be drawn, keeping in mind that the seismic response of this eleven-story structure is first-mode dominated (mass-participation coefficient of first-mode is 0.83): for lower level of drift demand with no structural nonlinearly, the optimal  $T_2$  to incorporate would be near the second-mode period of vibration of the structure. Note that at this level of drift demand the structure stays linear, an optimal  $T_2$  for  $R_{T_1,T_2}$  which can account for higher mode effect would be more efficient. And for higher level of drift demand such as  $\theta_{\max} \geq 0.01$ , then the optimal  $T_2$  will be larger than  $T_1$ . Note that for this drift demand level significant nonlinear behavior appears in the structure, and the fundamental period of the structure would be lengthened because of structural softening effect, so  $R_{T_1,T_2}$  with  $T_2$  values larger than  $T_1$  would be more efficient. For this eleven-story structure,  $T_2=1.5T_1$  is the best choice. It is also apparent that the fractional reduction in dispersion of  $S_a(T_1)_{cap}$  by using  $R_{T_1,T_2}$  for larger  $T_2$  values at high level of drift demand is much more significant than by using  $R_{T_1,T_2}$  for

smaller  $T_2$  values at low level of drift demand, which means that the impact of structural softening caused by nonlinearly on response is much more significant than higher mode effect. So  $R_{T_1, T_2}$  for  $T_2=1.5T_1$  is chosen as the second parameter of the vector to evaluate the fragility.

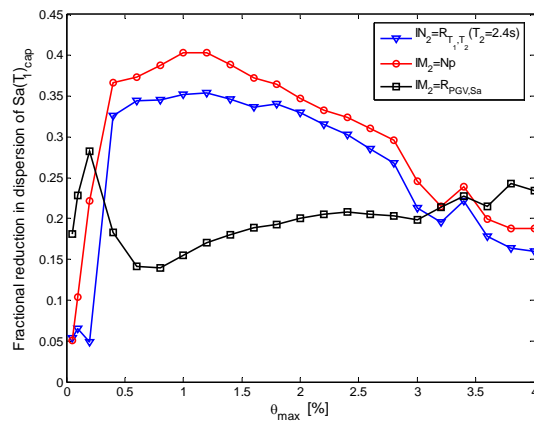


**Figure 4.5.** Fractional reduction in dispersion of  $S_a(T_1)_{cap}$  vs drift demand level by means of different vector-valued IMs

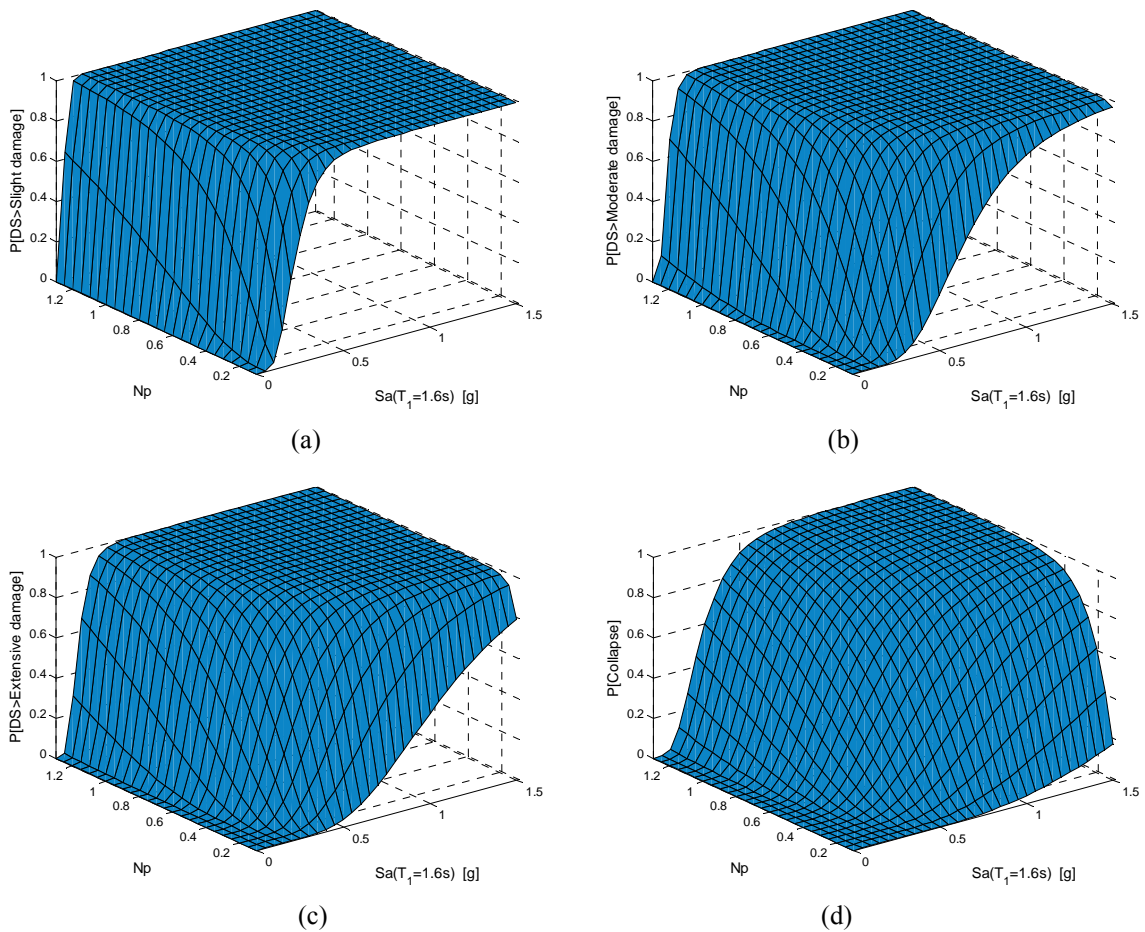


**Figure 4.6.** Fragility surfaces based on  $S_a(T_1) + Np$  for four damage levels: (a) slight damage; (b) moderate damage; (c) extensive damage; (d) collapse

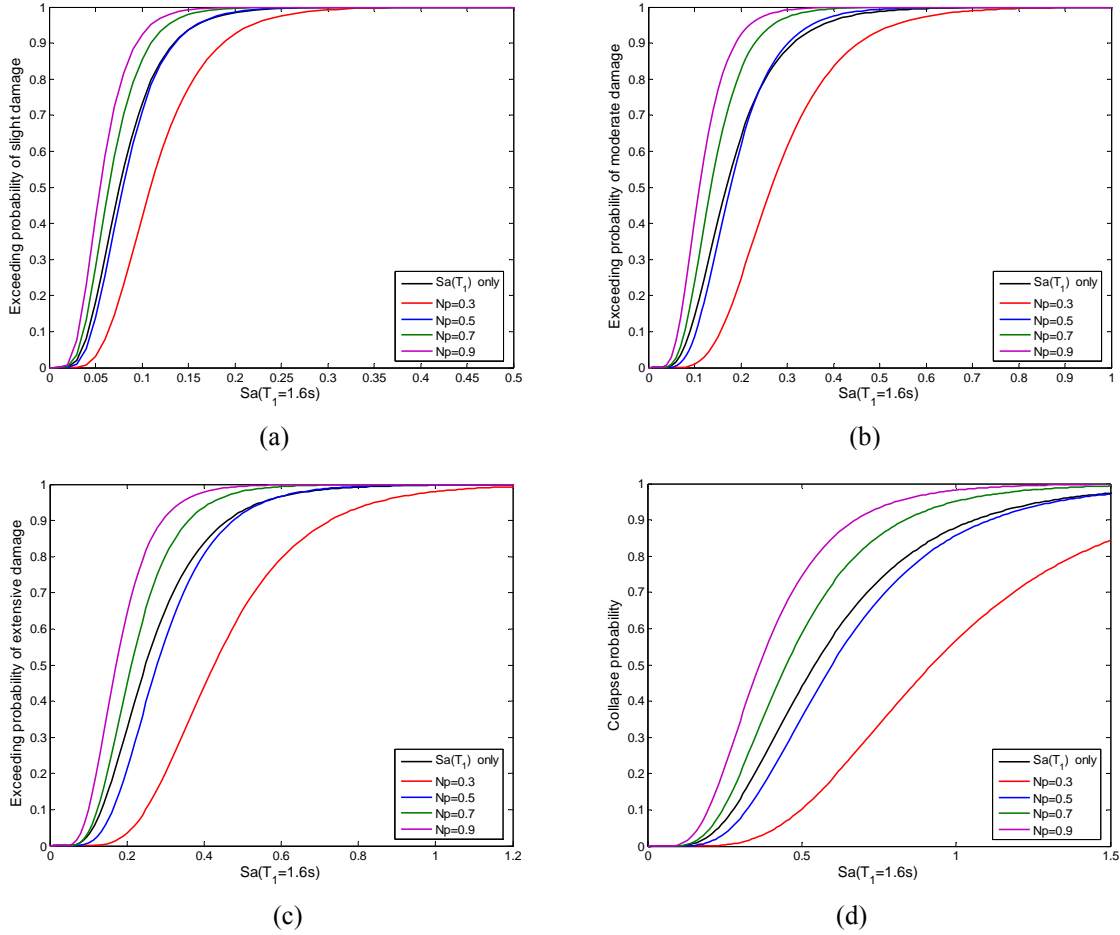


**Figure 4.7.**  $S_a(T_1)$  based fragility curves at different  $Np$  values: (a) slight damage; (b) moderate damage; (c) extensive damage; (d) collapse

Using the same method, fractional reduction in dispersion of  $S_a(T_1)_{cap}$  by means of  $Np$  and  $R_{PGV,S_a}$  is calculated. The efficiency of different IMs is compared, as shown in Figure 4.6. Here  $Np$  is calculated with the period between 1.6s and 3.2s based on the result in Figure 4.5. We find that  $Np$  is the most efficient parameter for a vector IM to evaluate the structural response, which indicates that spectra shape in a range of period larger than  $T_1$  is an important character of records for structural seismic demand analysis. It is apparent in Figure 4.4 that  $R_{PGV,S_a}$  shows less efficiency than  $Np$  and  $R_{T_1,T_2}(T_2 = 2.4s)$ .

Figure 4.6 shows the developed fragility surface based on a vector-valued IM:  $S_a(T_1)$  and  $Np$ . These surfaces can be visualized as fragility curves by projecting the surface onto the  $S_a(T_1)$  planes, as shown in Figure 4.7. These figures demonstrate the wide variation between fragility curves based on scalar-valued intensity measure, e.g.  $S_a(T_1)$ . Scalar-valued IM ( $S_a(T_1)$ ) based fragility curves can't incorporate the variability in ground motion as measured by another parameter,  $Np$ . It can be seen in Figure 9 that there can be a discrepancy of up to 70% between two curves (i.e., collapse probability of 10% for  $Np=0.3$  and 80% for  $Np=0.5$  at  $S_a(T_1)=0.5g$ ). The main advantage of fragility surfaces is that the variability of structural fragility due to a second parameter can be accounted for in contrast to when fragility curves are used. This means that which  $Np$  records should be used depends on the seismic hazard at the site when scalar-valued IM  $S_a(T_1)$  is used to evaluate the structural fragility. This information varies from site to site. Ignoring the effect of  $Np$  will ultimately bias the results. For example, if the seismic hazard disaggregation suggests that extreme motions are associated with records having a mean value of  $Np$  of about 0.9, but records are selected with a mean value of  $Np$  of

about 0.3, then the  $S_a(T_1)$ -based result will underestimate the seismic fragility. In other words, evaluation of structural fragility by means of vector valued IMs reduces the complexity of record selection procedure based on seismic environment (i.e., magnitude, distance, site conditions, etc.).

## 5 CONCLUSIONS

Alternative vector-valued IMs comprised of two ground motion parameters were used to present the ground motion potential. All the vectors considered here are based on  $S_a(T_1)$  (spectral acceleration at the first mode period of vibration of the structure) as the first parameters. As the second parameter of the vector, the peak ground velocity (PGV) and spectral shape parameters  $R_{T_1, T_2}$  and  $N_p$  were considered. The sufficiency and efficiency of these IMs were studied for medial-story RC frame structures and vector-valued IM based fragility surfaces were developed.

It is found that vector-valued IMs consisting of two parameters are more sufficient and efficient than scalar-valued IM  $S_a(T_1)$ . When  $R_{T_1, T_2}$  is used as the second parameter of the vector-valued IM, its sufficiency varies depending on the nonlinearity of the structure and the choice of  $T_2$ . At low level of drift demand the structure stays linear, an optimal  $T_2$  near the second mode period of the structure for  $R_{T_1, T_2}$  which can account for higher mode effect would be more efficient. For high level of drift demand, significant nonlinear behavior appears in the structure, and the fundamental period of the structure would be lengthened because of structural softening effect, so  $R_{T_1, T_2}$  with  $T_2$  values larger than  $T_1$  would be more efficient. For this eleven-story structure,  $T_2=1.5T_1$  is the best choice. It is also apparent that the impact of structural softening caused by nonlinearly on response is much more significant than higher mode effect. So  $R_{T_1, T_2}$  for  $T_2=1.5T_1$  is appropriate as the second parameter of the vector to evaluate the fragility.  $N_p$  calculated with the period between 1.6s and 3.2s shows the most efficient parameter for a vector IM to evaluate the structural response, which indicates that spectra shape in a range of period larger than  $T_1$  is an important character of records for structural seismic demand analysis. And  $R_{PGV, S_a}$  shows less efficiency than  $N_p$  and  $R_{T_1, T_2}(T_2 = 2.4s)$ . Fragility surfaces based on a vector-valued IM:  $S_a(T_1)$  and  $N_p$  are developed. The main advantage of fragility surfaces is that the variability of structural fragility due to a second parameter  $N_p$  can be accounted for in contrast to when fragility curves are used.

## ACKNOWLEDGEMENT

The financial support for this research provided by the specific fund of seismological industry in China (200808009) is appreciated.

## REFERENCES

- Baker JW and Cornell CA. (2005). A vector-valued ground motion intensity measure consisting of spectral acceleration and epsilon. *Earthquake Engineering and Structural Dynamics*. **34**, 1193-1217.
- Baker JW and Cornell CA. (2004). Choice of a vector of ground motion intensity measures for seismic demand hazard analysis. *Proceedings of the Thirteenth World Conference on Earthquake Engineering*. Paper No.:3384
- Cordova, P.P., Dierlein, G.G., Mehanny, S.S.F. and Cornell C.A. (2001). Development of a two parameter seismic intensity measure and probabilistic assessment procedure. *The second U.S.-Japan Workshop on Performance-Based Earthquake Engineering Methodology for Reinforce Concrete Building Structures*. 187-206.
- Dimitrios Vamvatsikos and C.Allin Cornell.(2002).Incremental dynamic analysis. *Earthquake Engineering and Structural Dynamics*. **31:3**, 491-514.
- D.M.Seyedi, P.Gehl, J.Douglas, et al. (2010). Development of seismic fragility surfaces for reinforced concrete buildings by means of nonlinear time-history analysis. *Earthquake Engineering and Structural Dynamics*. **39**, 91-108.
- Ellingwood BR. (2001). Earthquake risk assessment of building structures. *Reliability Engineering and System Safety*. **74:4**, 251-262.

- Fatemeh Jalayer and Cornell CA. (2006). Alternative non-linear demand estimation methods for probability-based seismic assessments. *Earthquake Engineering and Structural Dynamics*. **38:3**, 951-972
- Hwang HHM and Huo JR. (1994). Generation of hazard-consistent fragility curves. *Soil Dynamics and Earthquake Engineering*, **13**:345-354.
- Hwang HHM and Jaw JW. (1990). Probabilistic damage analysis of structures. *Journal of Structural Engineering* (ASCE). **116:7**, 1992-2007.
- Kafali C, Grigoriu M. (2004). Seismic fragility analysis. *Proceedings of the Ninth ASCE Specialty Conference on Probabilistic Mechanics and Structural Reliability*.
- Kafali C, Grigoriu M. (2007). Seismic fragility analysis: application to simple linear and nonlinear systems. *Earthquake Engineering and Structural Dynamics*. **36**,1885-1900.
- Luco N. (2002). Probabilistic seismic demand analysis, SMRF connection fractures, and near-source effects. *PhD Thesis*, Stanford University.
- Luco N, Manuel L, Baldava S and Bazzurro P. (2005). Correlation of damage of steel moment-resisting frames to a vector-valued set of ground motion parameters. *Proceedings of the Ninth International Conference on Structural Safety and Reliability (ICOSSAR'05)*. Rome, Italy.
- Prakash V, Powell G and Campbell S. (1993). DRAIN-2DX: basic program description and user guide, Report No. UBC/SEMM-93/17, University California at Berkeley, Berkeley, CA
- Rajeev P, Franchin P and Pinto PE. (2008). Increased accuracy of vector-IM-based seismic risk assessment. *Journal of Earthquake Engineering*. **12**,111-124.
- Schotanus MIJ, Franchin P, Lupoi A and Pinto PE. (2004). Seismic fragility analysis of 3D structures. *Structural Safety*. **26**, 421-441.
- Sei'ichiro Fukushima. (2010). Vector-valued fragility analysis using PGA and PGV simultaneously as ground-motion intensity measures. *Journal of Disaster Research*. **5:4**, 407-417
- Shinozuka M, Feng MQ, Lee J and Naganuma T. (2000). Statistical analysis of fragility curves. *Journal of Engineering Mechanics* (ASCE). **126:12**, 1224-1231.
- Shome N, Cornell CA, Bazzurro P and Carballo JE. (1998). Earthquakes, records, and nonlinear responses. *Earthquake Spectra*. **14:3**, 469-500.
- Song J and Ellingwood BR. (1999). Seismic reliability of special moment steel frames with welded connections: II. *Journal of Structural Engineering* (ASCE). **125:4**, 372-384.